Higher temperatures exacerbate effects of antibiotics on methanogenesis in freshwater sediment

Check for updates

E. Bollinger [1] ✉, P. Schwilden[1], F. Y. Lai[2], R. Schulz[1,3], M. Bundschuh [1,2] & S. Filker[4]

Methane (CH_4) emissions from natural systems are rising in a concerning manner with an incomplete understanding of its drivers. Recently, chemical stressors such as antibiotics have been suggested as a thus far overlooked factor increasing methanogenesis in freshwaters. Since usage and toxicological impact of antibiotics could increase in a warming climate, we assessed the temperature-dependence of antibiotic effects on methanogenesis. In this light, we conducted anaerobic incubations with freshwater sediment at 10, 15, and 20 °C in presence of a mixture of five antibiotics at field-relevant concentrations. Weekly measurements of CH_4 showed a strong temperature dependence of antibiotic effects by changing effect sizes, directions and dynamics. While antibiotics reduced CH_4 production at 10 °C, methanogenesis was elevated at 15 °C with the most pronounced increase occurring at 20 °C. Furthermore, antibiotics changed the prokaryotic assemblage at all temperatures and effect patterns of CH_4 producing Methanomicrobia strongly followed the patterns observed for methanogenesis. While analyses of compound-specific stable isotopes and the metatranscriptome suggest the acetoclastic pathway as most relevant, linking prokaryotic structure to function remains one of the most significant research challenges. Nevertheless, the evidence provided by this study suggests a positive relationship between temperature and the stimulating effects of antibiotics on CH_4 production.

Methane (CH_4) accounts for ~30% of the observed climate change despite atmospheric concentrations being much lower than those of carbon dioxide (CO_2)[1]. This is due to its substantially higher (28-fold) global warming potential compared to CO_2 and a ~260% higher atmospheric concentration (state of 2017) compared to pre-industrial times (i.e., 1750)[2]. Approximately 35–50% of released CH_4 originates from natural environments (369 Tg CH_4 yr^{-1}) with aquatic systems such as wetlands (147 Tg CH_4 yr^{-1}) and freshwaters (159 Tg CH_4 yr^{-1}) being the biggest contributors[2]. In their anaerobic sediments, microbial assemblages hydrolyze and ferment organic substrates before a specific group of archaea, the methanogens, produces CH_4[3]. Although the vast increases in atmospheric CH_4 concentrations post-2006 are to a large degree attributed to these natural sources[4], there is still a need to understand its precise causes. This is even more important given that emissions are projected to rise even further[5]. So far, researchers considered several global change pressures on methanogenesis such as eutrophication, increasing precipitation, and temperature feedbacks[5,6], but to a large degree ignored chemical stressors of anthropogenic origin, such as antimicrobial pharmaceuticals (i.e., antibiotics).

In freshwaters, antibiotics impact growth, performance, or survival of microorganisms relevant for central biogeochemical ecosystem processes[7]. Even though freshwater organisms are widely exposed to antibiotics[8], their effects on methanogenesis have mostly been studied in anthropogenic systems such as sewage sludge and biogas production systems (i.e., anaerobic digesters)[7]. However, results from these systems might not be transferable to the natural environment due to, for example, higher antibiotic concentrations, substrate quality and quantity, and temperatures exceeding 35 °C in most studies[7]. Little is known about the effects of antibiotics on CH_4 production in freshwater sediments. Among the limited studies, evidence points toward an increased release of CH_4 in the presence of antibiotics with changes in community composition and chemical environment being important drivers[9,10]. However, also more ambiguous responses were observed (i.e., positive and negative)[11], which makes further investigations all the more important.

[1]iES Landau, Institute for Environmental Sciences, RPTU Kaiserslautern-Landau, Landau, Germany. [2]Department of Aquatic Sciences and Assessment, Swedish University of Agricultural Sciences (SLU), Uppsala, Sweden. [3]Eusserthal Ecosystem Research Station, RPTU Kaiserslautern-Landau, Eusserthal, Germany. [4]Department of Ecology, RPTU Kaiserslautern-Landau, Kaiserslautern, Germany. ✉e-mail: eric.bollinger@rptu.de

At the same time, community compositions and chemical processes are temperature-dependent[12,13], which calls for the consideration of this factor in the light of global climate change[14,15]. The relevance of temperature as additional factor is substantiated by the often similar cellular responses to temperature and antibiotics in exposed organisms[16]: for example, chaperones (proteins assisting the conformational (un)folding of large proteins) are central for tolerance toward both temperature stress and antibiotics[17]. Furthermore, exposing prokaryotic cells to high temperatures protects them against subsequent exposure to antibiotics and vice versa[18–20]. Besides interactions at the toxicodynamic level, interactions between temperature and antibiotics can also be expected on uptake, elimination, and environmental fate[21]. This raises the question if the effects of antibiotics on methanogenesis are indeed temperature-dependent.

To address this knowledge gap, we exposed natural freshwater sediment to three field-relevant levels of an antibiotic mixture (i.e., amoxicillin, ciprofloxacin, erythromycin, sulfamethoxazole, and tetracycline at sum concentrations of 0, 5, and 5000 μg L^{-1}) at three temperatures (10, 15, and 20 °C) under anaerobic conditions. While average lake temperatures rose 0.34 °C per decade between 1985 and 2009[22], the temperature steps are chosen with small and shallow ponds in mind[23] as these excessively emit CH_4[24]. Furthermore, also other anthropogenic activities such as discharge of heated water, removal of water or riparian vegetation justify the focus on higher temperature alterations[25]. According to previous studies on freshwater communities[9,10], we hypothesized to observe an increased CH_4 production in presence of antibiotics. We further assumed higher effects of antibiotics with increasing temperature, since a large body of research showed a positive connection of temperature and the toxic action of many chemicals[21]. Aiming for mechanistic insights, we involved compound-specific stable isotope analysis to discriminate between utilized substrates, 16S rRNA metabarcoding for microbial community assessment, and metatranscriptomics to understand functional responses.

Material and methods
Experimental setup
The experimental design largely followed the setup established by Bollinger et al.[9]. Briefly, pristine sediment was sampled from the top ~20 cm of a pond on the premises of the Eusserthal Ecosystem Research Station (EERES). The pond is located within the biosphere reserve Palatinate Forest-Northern Vosges upstream from anthropogenic impacts such as agriculture and wastewater treatment plants. In the laboratory, a wet weight of 10.21 ± 0.26 g sediment was spiked with 20 g kg^{-1} powder of black alder leaves (*Alnus glutinosa*) to increase substrate availability. Subsequently, 30 mL of unfiltered pond water (adjusted to pH 7 and containing the respective antibiotic treatment, see section "Antibiotic treatment and analysis") were added to crimp top incubation glasses to create a slurry. The headspace was flushed with N_2 and tightly sealed with butyl septa to ensure nearly anaerobic conditions. The test systems (n = 26) were randomly placed in total darkness in a climate cabinet (Mytron Bio- und Solartechnik GmbH, Germany) at 10, 15, and 20 °C (Fig. S1) for a total duration of 27, 12, and 11 weeks, respectively. The difference in study duration among temperatures was motivated to increase comparability because methanogenic activity will be less at the lower temperatures. The end of the experiment was set to a system state when CH_4 headspace concentration rose less than 1% per day (approximately stagnation, see section "Statistics"). For molecular analyses, six replicates of sediment were retrieved (shaken and turned upside down on a centrifuge tube to extract as much sample as possible) and stored at −80 °C at the end of the experiment as well as the beginning of the exponential phase (i.e., when CH_4 production rates doubled, see section "Statistics"), which were 15, 6, and 4 weeks at 10, 15, and 20 °C, respectively.

Antibiotic treatment and analysis
Antibiotics cover a wide range of modes of action and several classes are of high environmental relevance. For this reason and to increase comparability with our previous study, we used the same five-component mixture that was introduced by Bollinger et al. (Table S1)[9] with equal mass fractions at sum

concentrations of 0, 5, and 5000 μg L^{-1} (referred to as control, low and high). While the low concentration is highly field-relevant (cf. the meta-analysis by Danner et al[8].), the high concentration reflects extreme cases[26]. As mentioned above, natural pond water was used for the dilution series to provide realistic levels of nutrients. To ensure a successful initial exposure and observe potential degradation, water samples for analyses of antibiotic concentrations were taken at test start, in the middle and the end of the experiment and stored at −80 °C until further analysis.

Sample preparation and chemical analysis followed the procedure of our previous study[9]. In brief, after centrifuging the water samples (2 mL) at 8000 rpm for 5 min at 7 °C, an aliquot (150 μL) was transferred to amber vials followed by spiking with mass-labeled internal standards (20 μL of 500 μg L^{-1}) and methanol (30 μL). Chemical analysis was done via direct injection (4 μL) onto a system of liquid chromatograph (ExionLC™ AD UHPLC) coupled with tandem mass spectrometry (SCIEX Triple Quad™6500$^+$). Antibiotics were chromatographically separated on a biphenyl analytical column (100 × 2.1 mm, 2.6 μm, Phenomenex Kinetex®) with Milli-Q water and methanol as mobile phase, each with 0.1% formic acid. A nine-point calibration curve was analyzed three times throughout sample analysis with linearities of more than 0.996 (amoxicillin: 0.9994, ciprofloxacin: 0.9960, erythromycin: 0.9992, sulfamethoxazole: 0.9992, tetracycline: 0.9990). Chemical concentrations were corrected with responses of the internal standards to compensate for instrumental variations and matrix effects. Spiked water samples with the target compounds resulted in the average recovery (n = 7) of 94 ± 9.0, 103 ± 4.4, 97 ± 4.2, 98 ± 4.7, and 50 ± 9.3% for amoxicillin, ciprofloxacin, erythromycin, sulfamethoxazole, and tetracycline, with their limits of quantification (LOQ) estimated at 0.4, 5.0, 0.4, 0.15, and 0.7 μg L^{-1}. Measurements suggest a valid setup of the experiment (i.e., a separation factor of ~1000 between the low and high treatment) despite a ready degradation of the used compounds (i.e., 47–87% of nominal concentration at test start and predominantly below LOQ in the middle and end of the incubation, Table S2).

Greenhouse gas measurements
For each incubation system, 100 μL of headspace volume (V_i) were analyzed weekly for their CH_4 and CO_2 concentration using a closed-loop with a cavity-enhanced laser absorption spectrometer (UGGA, model 915-0011, Los Gatos Research Inc., USA). To calculate the mole fraction in the headspace (x_h), the equilibrium mole fraction (x_e, ppm) of the sample gas and loop gas was corrected for the loop volume (V_l, determined with reference gas of certified levels of CH_4 and CO_2, Messer Industriegase, Germany) and the mole fraction of the background gas (x_0)

$$x_h = \left(\frac{V_l}{V_i}\right) \cdot (x_e - x_0) + x_e \qquad (1)$$

The dissolved amount of CH_4 and CO_2 (n_w) was calculated using Henry's law

$$n_w = K_H \cdot x_h \cdot V_w \cdot f_1 \qquad (2)$$

where V_w is the volume of water, f_1 is a conversion factor (10^{-1} Pa ppm^{-1}) and K_H is the temperature-adjusted Henry constant[27,28] of CH_4 and CO_2 calculated as

$$\ln\left(K_{H_{CH_4}}\right) = -115.6477 + 155.5756\left(\frac{T_K}{100}\right)^{-1} + 65.2553 \cdot \ln\left(\frac{T_K}{100}\right) - 6.1698\left(\frac{T_K}{100}\right) \qquad (3.1)$$

$$\ln\left(K_{H_{CO_2}}\right) = -58.0931 + 90.5069\left(\frac{T_K}{100}\right)^{-1} + 22.294 \cdot \ln\left(\frac{T_K}{100}\right) \qquad (3.2)$$

where T_K is the temperature in Kelvin. The amount of CH_4 and CO_2 was ultimately normalized to the dry weight of sediment in the system

$$c(CH_4, CO_2) = \frac{n_w + (x_h \cdot V_h \cdot f_1) \cdot (R \cdot T)^{-1}}{m_s \cdot \left(1 + \Theta_g\right)^{-1}} \qquad (4)$$

where V_h is the headspace volume, R is the universal gas constant, m_s and Θ_g are the wet weight and the gravimetric water content of the sediment (i.e., the mass of water per mass of dry sediment), respectively.

Compound-specific isotope ratio measurements

Once a week, the compound-specific isotope ratio of five replicates per treatment was determined by injecting headspace into a gas chromatograph (GC, Trace GC Ultra, Thermo Fisher Scientific, Germany) at 32 °C equipped with a capillary column (length: 27.5 m, internal diameter: 0.32 mm, film thickness: 10 µm, Agilent J&W PoraPLOT Q, USA) and coupled to a GC IsoLink combustion oven and a ConFlo IV that connects to a Delta V Advantage isotope ratio mass spectrometer (IRMS, Thermo Fisher Scientific, Germany). The injection volumes were adjusted to the sample concentration of CH_4 and CO_2 to ensure a constant peak area. Isotope ratios are expressed using the δ-notation against Vienna Pee Dee Belemnite (VPDB).

$$\delta^{13}C = \left(\frac{R_{sample}}{R_{reference}} - 1\right) \cdot 1000\text{‰} \qquad (5)$$

These values can be used to calculate a fractionation factor

$$\alpha_c = \frac{\delta^{13}C - CO_2 + 1000}{\delta^{13}C - CH_4 + 1000} \qquad (6)$$

Since CH_4 is mainly produced from CO_2 and H_2 (i.e., hydrogenotrophic methanogenesis, HM) and acetate (i.e., acetoclastic methanogenesis, AM) and enzymes involved in these processes show distinct affinities towards ^{12}C and ^{13}C, the fractionation factor can be used to infer which substrate is predominantly used (i.e., higher values indicate more HM)[29].

RNA extraction and processing

RNA was extracted from 2 g sediment of each of the six replicate samples (see section "Experimental setup") using Qiagen's RNeasy PowerSoil Total RNA kit following the manufacturer's guidelines. RNA concentrations were measured using a Nanodrop2000 (Thermo Fisher Scientific, Germany) and RNA integrity was assessed on an Agilent Bioanalyzer 2100 system.

Metabarcoding

For prokaryotic community analysis, 2 µl RNA extract of each replicate were reverse transcribed into cDNA using the random primers supplied by the iScript synthesis kit (BioRad). The hypervariable V4 region of the 16S rRNA gene was used as target marker gene employing the primer pair 515Fm (5′-GTGYCAGCMGCCGCGGTAA-3′) and 806Rm (5′-GGACTACNVGGGTWTCTAAT-3′)[30]. For the amplification of the marker gene, 2 µl of cDNA were used as a template for each replicate. The PCR protocol consisted of an initial activation step at 98 °C for 30 s, followed by 26 cycles consisting of 98 °C for 10 s, 63 °C for 30 s, and 72 °C for 30 s, and a final extension for 5 min at 72 °C. To minimize PCR bias, three individual PCR reactions for each of the samples were prepared. Afterwards, these replicate samples were pooled and subjected to library preparation using the Next Ultra DNA Library Prep Kit for Illumina (NEB, USA). The quality of the final libraries was assessed with an Agilent Bioanalyzer 2100 system. Libraries were sequenced on an Illumina MiSeq platform, generating 2 × 300 nt paired-end reads by StarSeq, Mainz, Germany.

Resulting raw reads were processed as described in Bollinger et al.[9]. Briefly, primer stretches were removed from the raw reads using cutadapt v1.18[31]. Reads were then subjected to the DADA2 pipeline[32] implementing the following criteria: truncLen = c(192, 217), maxEE = 1, maxN = 0 and minOverlap = 20. Processed reads were submitted to chimera identification and removal using vsearch v2.13.7[33]. Taxonomy was assigned to resulting amplicon sequence variants (ASVs) using the SINTAX algorithm[34] against the Greengenes database v13.5[35]. After merging the ASV-contingency table with the taxonomic information, ASVs without any taxonomic assignment and ASVs which occurred less than five times across all samples, and thus, may be artifactual sequences[36] were removed. The resulting ASV-to-sample matrix was then used for downstream statistical analyses (see section "Statistics").

Gene expression profiling (metatranscriptomics)

Around 2 µg of total RNA of each sample were used as starting material for the gene expression profiling. To enrich messenger RNA in prokaryotic samples, an rRNA depletion was performed using the NEBNext rRNA Depletion Kit for Bacteria following the manufacturers' instructions. Afterwards, the NEBNext Ultra II Directional RNA library Kit was used for sequencing library preparation. Quality-checked libraries were then sequenced on an Illumina NextSeq 2000 machine, generating 2 × 150 nt reads by StarSeq, Mainz, Germany.

Quality of the resulting raw reads was first checked and visualized using FastQC[37] and MultiQC[38]. All reads were then processed using Trimmomatic v0.39[39] with the following parameters: ILLUMINA-CLIP:NexteraPE-PE.fa:2:30:10, LEADING:3, TRAILING:1, SLI-DINGWINDOW:4:20, and MINLEN:50. Residual rRNA fragments were filtered out and removed with SortMeRNA v4[40] run with default settings. mRNA reads were subjected to Trinity v2.15.1[41] for contig assembly. KEGG functional assignment of the resulting contigs was done in the SqueezeMeta v1.6.3 pipeline[42].

Statistics

In anoxic incubations, methanogenesis usually shows three distinct phases: (1) an almost linear phase where methanogenesis is limited by available electron acceptors in the sediment (i.e., other metabolic pathways are thermodynamically preferential), (2) an exponential phase where CH_4 production is mainly limited by the activity of methanogenic archaea, and (3) a stagnation phase where production rates are limited by the depletion of easily available substrate and consequently drop[43]. This progression of growth phases over time (t, in days) can be described by a generalized logistic function[44].

$$CH_4(t) = A + \frac{L - A}{\left(1 + ve^{-k(t-\tau)}\right)^{\frac{1}{v}}} \qquad (7)$$

The parameters A and L set the initial and final concentrations of the curve, k and τ describe the kinetics of the methanogenesis, while v affects the symmetry of the curve. The parameter k depends on how quickly L (mostly dependent on available substrate, which is equal among all treatments and thus not of primary relevance for effects of antibiotics) is reached, whereas τ describes how fast the inflection point of the curve is reached (i.e., it covers the two phases that are mostly determined by microbial processing). Since the focus of this study was biologically mediated alterations on CH_4 production, we used effects on parameter estimates for τ as endpoint of toxicity that best describes the processing/kinetics of the assessed microbial assemblages. These models were built with non-linear Bayesian regression using the R (version 4.3.1)[45] package "brms" (version 2.20.4, chains: 4, iterations: 20,000, thinning: 10, warmup: 16,000)[46] that utilizes "rstan" (version 2.32.3)[47]. For the chains to run properly, prior distributions of the parameters were chosen, which

was done separately for each temperature.

$$L \sim Normal\left(\mu\left(CH_4\left(t = t_{max}\right)\right), \sigma\left(CH_4\left(t = t_{max}\right)\right) \cdot 5\right) \quad (8.1)$$

$$A \sim Exponential(1) \quad (8.2)$$

$$k \sim Exponential(1) \quad (8.3)$$

$$v \sim Normal(1, 1) \quad (8.4)$$

$$\tau \sim Uniform\left(0, t_{max}\right) \quad (8.5)$$

$\mu\left(CH_4\left(t = t_{max}\right)\right)$ and $\sigma\left(CH_4\left(t = t_{max}\right)\right)$ are mean and standard deviation of CH_4 concentrations of the control at test termination (t_{max}). These priors aimed at being informative enough to warrant a convergence of the chains and thus a proper fit of the models but unspecific enough to not bias their outcome. The latter was verified by running sensitivity analyses (i.e., analyzing how the posterior is changed by altering the prior, Fig. S2). Furthermore, the validity of the model was tested by generating simulated data sets and comparing generatively introduced effects with estimated effects by the model (Fig. S3). To generate these data sets, we used the generalized logistic function described above to set the mean and defined the standard deviation as

$$\sigma = f_{scale} \cdot \left(k \cdot (L - A) \cdot e^{-k \cdot (d-\tau)} \cdot \left(v \cdot e^{-k \cdot (d-\tau)} + 1\right)^{-\frac{1}{v} - 1}\right) \quad (9)$$

where f_{scale} is a scaling factor estimated with non-linear least squares with the measured σ as response and the parameters k, L, A, τ, and v from the respective model. The rest of the equation is the first derivative of the generalized logistic function. The validity tests revealed an accuracy of 0.05% and a precision of 0.35%.

To estimate the uncertainty of observed differences in τ between treatments, we calculated contrasts of the posterior distribution as effect in percent. Posterior distributions will be addressed with the maximum a posteriori estimate (MAP) and the 95%-confidence highest-density credible interval (HDI). The posterior odds of negative and positive values will be referred to as Bayes factor (BF) and express the likelihood of H_1 (e.g., there is a difference between treatments) versus the likelihood of H_0 (e.g., there is no difference between treatments) given the data. The BF was expressed as >1 regardless of the effect direction for better readability and comparability. If all comparisons are in favor of H_1 over H_0 (or vice versa) the BF is infinite (i.e., Inf).

Relative abundances from metabarcoding analyses were expressed relative to the respective control (ΔRA) of the same treatment combination to make effects more comparable between time points and temperatures. For an arbitrary taxonomic level this was done as

$$\Delta RA = \frac{\sum_{i=1}^{n} RA_{Ti} - RA_{Ci}}{\sum_{i=1}^{n} RA_{Ci}} \quad (10)$$

where RA_{Ti} and RA_{Ci} are the relative abundance of ASV i in the treatment and control, respectively. Non-metric multidimensional scaling (NMDS) was done on Hellinger transformed relative abundances based on Bray–Curtis dissimilarities using the R package "vegan" (version 2.6-4)[48]. The significance of these dissimilarities was tested with permutational multivariate analysis of variance (PERMANOVA)[49]. The species contributions to between-group dissimilarities were calculated with SIMPER. Metatranscriptional data was analyzed as transcripts per million using the R package "SQMtools" (version 1.6.3)[50]. Data and code are freely available at https://zenodo.org/doi/10.5281/zenodo.12582590. The metabarcoding and metatranscriptome sequence data were deposited in NCBI's BioProject database under BioProject ID PRJNA1127245.

Results
Methane production
Across all temperature and antibiotic treatments, CH_4 concentration followed a generalized logistic growth (Fig. S4). In the controls, the achievement of the inflection point of methanogenesis (τ) changed from 155.2 d (152.9–157.2) at 10 °C to 66.3 d (65.7–66.9) at 15 °C and 36.6 d (36.1–37.1) at 20 °C. While at the low antibiotic concentration τ differed only moderately from the control (MAP of 0.04, −0.85, and −0.69% and BF of 1.2, 9.1, and 2.8 at 10, 15, and 20 °C, respectively), effects were more pronounced in the high antibiotic treatment (Fig. 1). More specifically, τ was 9.1% (6.6–11.4) slower at 10 °C (BF = Inf), 2.4% (1.1–3.7) faster at 15 °C (BF = 1599) and 7.9% (5.0–10.0%) faster at 20 °C (BF = Inf). The CH_4 concentrations in the headspace over time showed distinct effect patterns between temperatures. At 10 °C, CH_4 concentrations at the high antibiotic treatment were higher in the first stage of the incubation and became lower in the exponential growth phase (relative to the control). At 15 °C, CH_4 concentrations at the high antibiotic treatment were consistently higher than in the control. At 20 °C, CH_4 concentrations in the high antibiotic treatment were lower in the initial phase of the incubation and then superseded the control in the exponential growth phase. Therefore, temperature did affect the effects size, direction, and dynamics of antibiotics on methanogenesis.

Stable isotopes
Across all temperatures, $\delta^{13}C$ values of CH_4 were initially low and stayed relatively constant until the beginning of the exponential phase in which values quickly rose (Fig. 2). $\delta^{13}C$ values of CO_2 generally started relatively low, increased in the beginning of the first stage of incubation and have come to a relatively constant low value until the beginning of the exponential phase. The same pattern was reflected in the fractionation coefficient α_C, which is a function of both $\delta^{13}C–CH_4$ and $\delta^{13}C–CO_2$. Statistically strong differences compared to the control (i.e., BF > 30) occurred at weeks 1, 3, and 5 at 20 °C, week 2 at 15 °C, and weeks 2, 4, 19, 20, 22, and 23 at 10 °C.

Metabarcoding
A total of 5046 ASVs from 52 phyla, 109 classes, and 157 orders were analyzed with an average of 779 ± 190 ASVs across $69,430 \pm 16,751$ reads per sample. Across all prokaryotes the assemblage differed significantly between temperatures, antibiotic concentrations, and time of sampling (i.e., mid and end, $p < 0.0001$, Fig. 3). Changes in assemblages were mostly detected at the high antibiotic concentration. Across both time points, the classes that contributed the most to average dissimilarities between the high treatment and control were Clostridia (19.9%, 15.0%, and 12.0% at 10, 15, and 20 °C, respectively), Bacteroidia (10.2%, 9.9%, and 12.0% at 10, 15, and 20 °C, respectively), and Bacilli (4.9%, 4.5%, and 4.2% at 10, 15, and 20 °C, respectively). While ASVs of Clostridia showed on average an increase of up to 100% in relative abundance, ASVs of Bacilli almost completely vanished in the high antibiotic treatment. ASVs of Methanomicrobia, the class that contains most methanogenic Archaea, also showed considerable effect sizes that match the observations in CH_4 production (i.e., negative effects at 10 °C and positive effects at 15 and 20 °C in the exponential phase of the incubation). However, the overall moderate relative abundance of these ASVs results in dissimilarity contributions of up to 2.5%.

Within the phylum of Euryarcheota, effects of antibiotics on the assemblage were less pronounced compared to the whole prokaryotic assemblage ($p = 0.0717$), but effects of temperature and time of sampling were highly significant ($p < 0.0001$). Again, effects were higher at the high concentration and the most relevant family for between-treatment dissimilarities (across both time points) was Methanosarcinaceae with contributions of 24.0%, 18.1%, and 14.5% at 10, 15, and 20 °C, respectively.
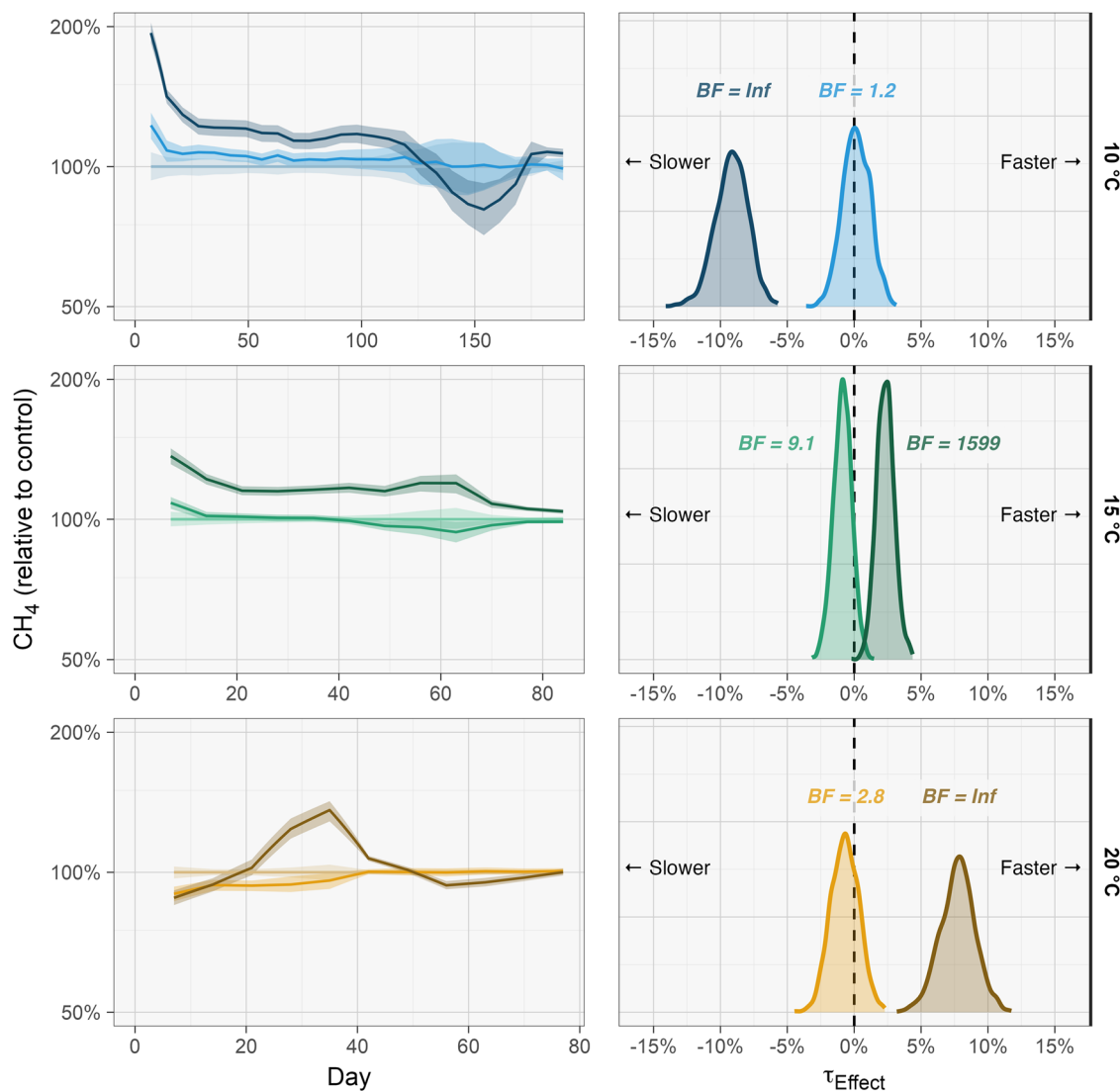
Fig. 1 | CH$_4$ concentrations relative to the control (=100%; mean with 95% confidence interval, left panels) and posterior density of the kinetic parameter τ as effect relative to the control (right panels). Temperatures are indicated by the hue (i.e., color type, blue: 10 °C; green: 15 °C; yellow: 20 °C) and concentrations of antibiotics by the lightness (light: 0 µg L^{-1}; medium: 5 µg L^{-1}; dark: 5000 µg L^{-1}). The Bayesian factor (BF) indicates the odds of the probabilities of τ_{Effect} being greater than zero and τ_{Effect} being smaller than zero (and vice versa as it is always expressed as >1).

Gene expression analysis

Across all samples, we found transcripts from 9843 KEGG functional orthologs, while 79.5% of transcripts were unclassified. Of these remaining transcripts (analyzed as transcripts per million), 6.5% were associated with methane metabolism (KEGG pathway ec00680). Within this pathway, the methyl-coenzyme M reductase (MCR) subunits alpha (11.7%), beta (7.3%), C (6.4%), gamma (6.3%), and D (4.6%) were the most expressed making up 36.3% of transcripts. The three next most transcribed enzymes were enolase (6%), acetyl-CoA decarbonylase/synthase (ACDS) complex (12.7% across four subunits) and acetate kinase (2.3%). Overall, transcripts of the methane metabolism pathway were relatively higher expressed at the end of the incubation at 10 and 15 °C, while being at a comparable level to the middle of the incubation at 20 °C (Fig. 4).

While at 10 °C MCR was downregulated in the middle of the incubation at the high antibiotic concentration, it was upregulated at 15 °C and constant at 20 °C. Transcripts of the ACDS complex followed the same pattern. Apart from that, the enzymes with the most notable downregulated transcripts were enolase, phosphate acetyltransferase, methanol--corrinoid protein co-methyltransferase, methanol corrinoid protein, and malate dehydrogenase.

Discussion

Temperature increases the effects of antibiotics on methane production

For the assessed microbial assemblage, kinetics of CH$_4$ production indicates a positive interaction between temperature and toxic action of antibiotics. While at 20 °C, our results consolidate the evidence for the enhancing effects of antibiotics on methanogenesis[9,10], effect sizes become lower at 15 °C and eventually negative at 10 °C. Interestingly, not only the effect sizes and directions changed with increasing temperature, but also the effect patterns over the course of the incubation. Most notably, antibiotics increased methanogenesis at 10 °C but decreased it at 20 °C in the early stages of the incubation. At this stage, CH$_4$ concentrations are limited by both aerobic (due to incomplete removal of O$_2$) and anaerobic oxidation (using electron acceptors other than O$_2$)[51] as well as competition for H$_2$[3]. Altered CH$_4$ concentrations could thus be a consequence of effects on either of these processes. Process-altering effects can be explained in both directions with current toxicodynamic knowledge. For example, prokaryotes can cope with a stressor by keeping metabolic rates to a minimum (i.e., dormancy)[52], which could explain the initially lower CH$_4$ concentration in the high
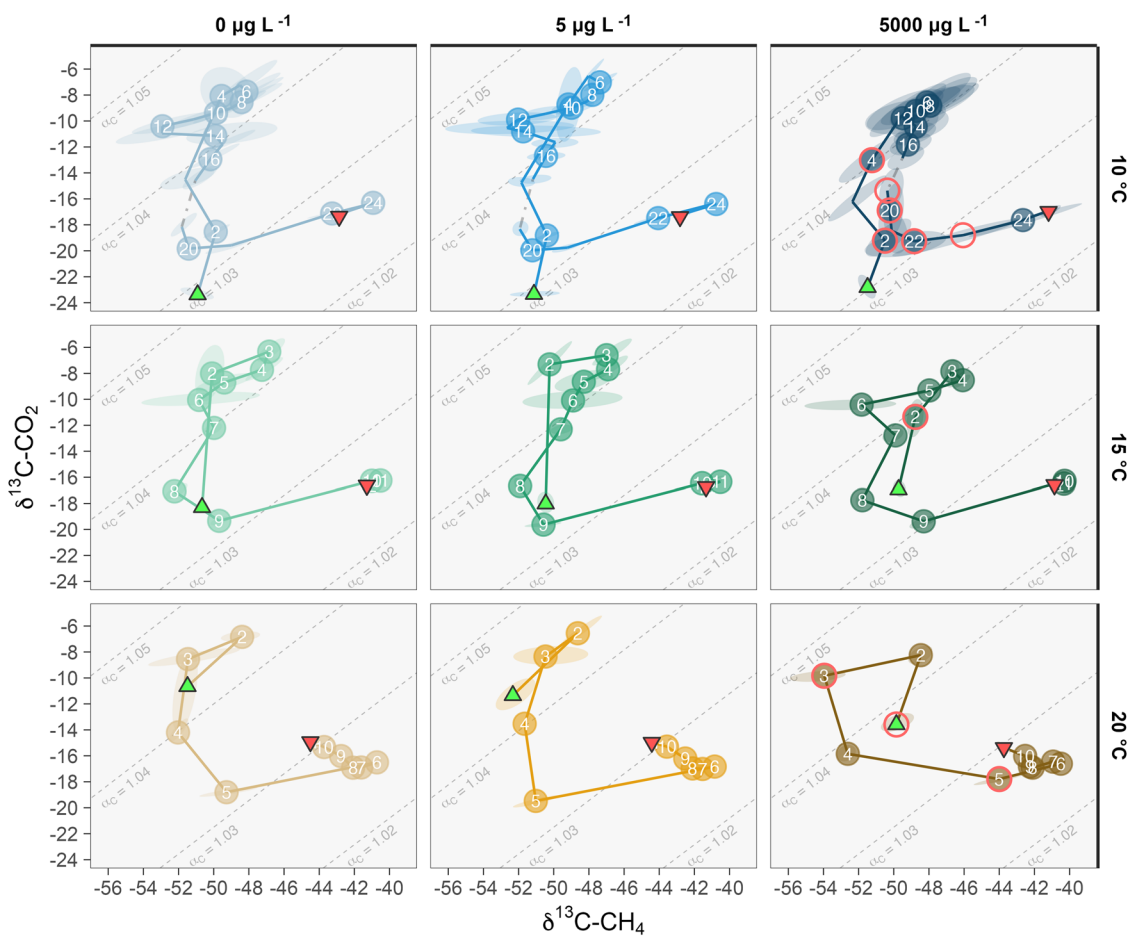
Fig. 2 | Compound-specific stable isotope ratios of C for CO_2 and CH_4 over the course of the experiment. Week numbers are added to each node in the path and start/end are depicted as green and red triangle, respectively. A 50% confidence ellipse is plotted to display variability in the data. Points are enclosed by red circles if either CH_4 or CO_2 were distinct from the control (i.e., Bayesian factor >30) at the respective day and temperature. Rows show different test temperatures and columns different concentrations of antibiotics. Temperatures are further indicated by the hue (i.e., color type, blue: 10 °C; green: 15 °C; yellow: 20 °C) and concentrations of antibiotics by the lightness (light: 0 µg L^{-1}; medium: 5 µg L^{-1}; dark: 5000 µg L^{-1}). Since no measurement was taken in week 18 due to technical issues, a gray dashed line was added to connect the measurements of weeks 17 and 19. Dashed gray lines of constant fractionation factor are plotted to ease the interpretability of the dominant form of methanogenesis (higher: more hydrogenotrophic methanogenesis, lower: more acetoclastic methanogenesis).

antibiotic treatment at 20 °C. Another bacterial defense mechanism is the excretion of extracellular polymeric substances (EPS), which could be used by methanogens[53] and thus points toward the initially positive effects observed at 10 °C. The production of EPS is a rather primary defense mechanism[54] while dormancy is indicative of more severe and/or persistent stress[55]. Since factors that drive toxicity changes at different temperatures are as diverse as altered toxicokinetics, homeostasis, or metabolism (reviewed by Noyes et al.[21]), no plain prediction can be made ad hoc. However, the tendency of higher toxicity with increasing temperature might at least provide indications of the above-hypothesized mechanisms of EPS excretion (potentially promoting methanogenesis) and dormancy (potentially inhibiting methanogenesis).

Contrary to what was observed in the initial stage of incubation, an effect in the opposite direction (i.e., negative at 10 °C and positive at 20 °C) was observed during the exponential phase. Zhang et al.[10] hypothesized the development of resistance[56,57] to explain the highest effects being seen in a later stage of incubation. However, running a basic local alignment (BLAST) of our metatranscriptome data against the Comprehensive Antibiotic Resistance Database (CARD)[58] did not show any indication for this hypothesis (Fig. S5). Nevertheless, these later-stage effect patterns might also occur solely because of a protraction of toxic effects from the early stages of incubation. More specifically, the effects of antibiotics may have been protracted due to changes in the

composition of the prokaryotic assemblage, which in turn altered substrate availability. This hypothesis is based on measured antibiotic concentrations being <0.5% of the nominal start concentration (Table S2) during the exponential phase of incubation. Hence, the direct action of antibiotics is assumed to be minor during this and later phases of the experiment. Differences in substrate composition, as a consequence of altered metabolic processes in the beginning of the experiment, could have been represented by changes in the stable isotope ratios of CH_4 and CO_2. Although an antibiotic treatment effect on signatures at the high concentration was present at all temperature regimes, these alterations occurred at varying stages of the incubation and the general trajectory across the biplot was comparable between antibiotic concentrations. It is important to note that while the stable isotope approach yields valuable mechanistic process-oriented information (i.e., based on mass balance), it is not very sensitive given that the multitude of substrates cannot be resolved by a two-dimensional tracing system and only the terminal step of methanogenesis is considered. This means that while the observed differences could most likely be explained by the changes in kinetics and dynamics of methanogenesis[9], more subtle changes or changes on metabolically more distant steps are possible (see sections "Assemblage alterations" and "Transcriptional alterations") and might be relevant to explain the time dependence of effect patterns.
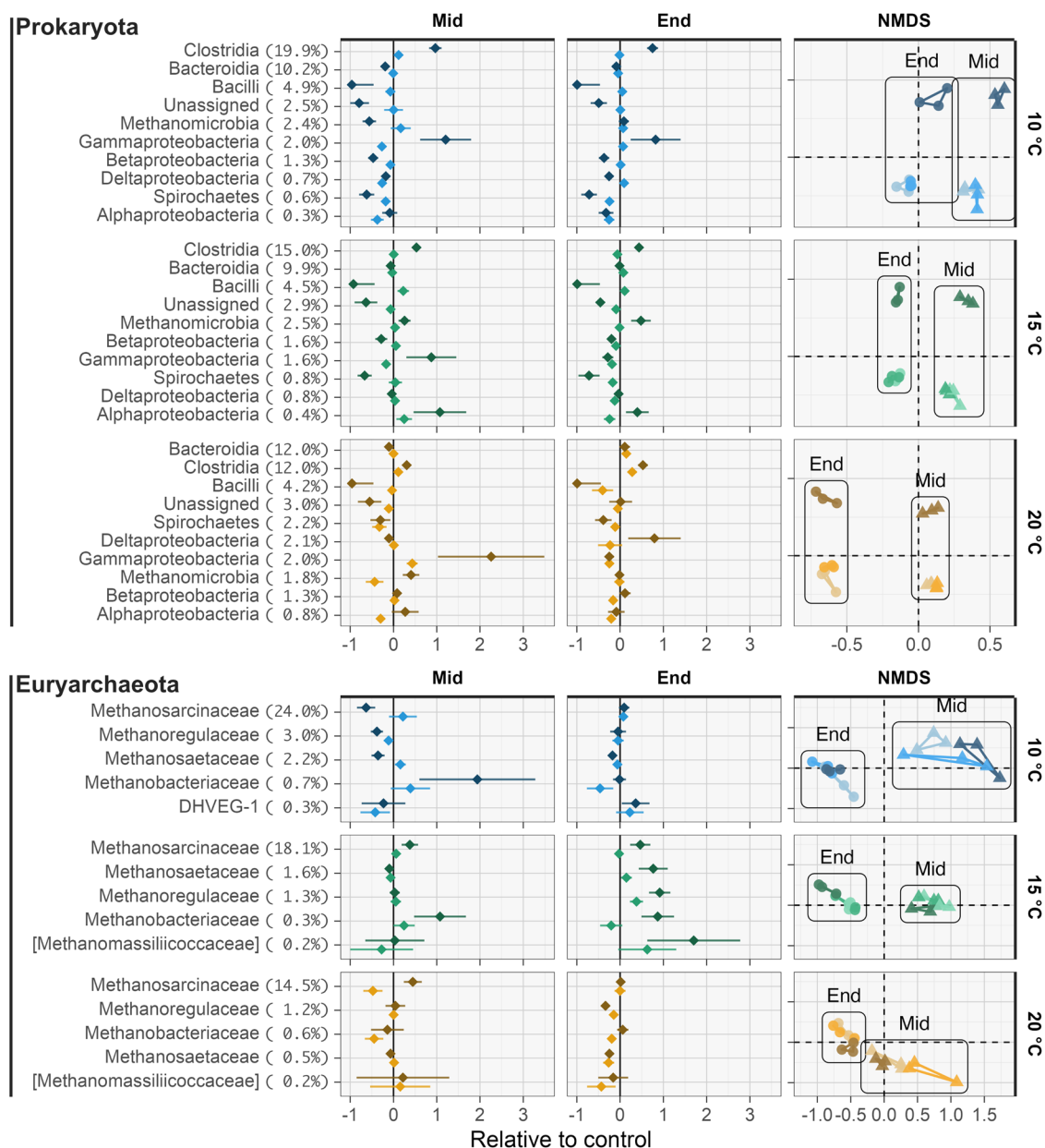
Fig. 3 | Metabarcoding community analyses for all prokaryotes and the phylum Euryarchaeota. The left and middle columns show average changes in relative abundance to the control normalized to the average relative abundance in the control (in relative change ± SE) for classes of prokaryotes and families of Euryarchaeota at the middle (left column) or end (middle column) of the experiment. Negative values indicate reductions in relative abundance, while positive values represent increases in relative abundance. The taxonomic levels are ordered by their contribution to the dissimilarity between the high concentration and the control (averaged for both time points), which is printed next to the taxonomic level in parentheses. The right column shows NMDS plots based on Hellinger transformed relative abundances for prokaryotes (stress: 0.048) and Euryarchaeota (stress: 0.036). Assemblages from different temperature treatments but same taxonomy (i.e., prokaryotes and Euryarchaeota) share the same ordination space to improve comparability. Temperature treatments are distinguished by the hue (i.e., color type, blue: 10 °C; green: 15 °C; yellow: 20 °C) and concentrations of antibiotics by the lightness (light: 0 µg L^{-1}; medium: 5 µg L^{-1}; dark: 5000 µg L^{-1}).

Assemblage alterations

While the whole prokaryotic assemblage at the high antibiotic concentration is vastly different from the control at all temperatures and time points, effects on the archaeal kingdom Euryarchaeota, although trending toward significance, were less pronounced. This finding is in line with the assumption that antibiotics have lower effects on Archaea and thus indicates that alterations in the assemblage and functioning of methanogens are dominantly indirect[59]. These indirect links can, for example, be mediated by syntrophic/amensal/competitive interspecific relationships[60] and by resulting changes in available substrates/metabolic products. Even though our methodology is state of the art in terms of accuracy and specificity, attempting to explain individual decreases/increases in specific taxon

abundance by presumed interspecific relationships is oversimplified as the number of these interactions increases quadratically with the number of taxa and cannot be causally isolated in such a complex community.

Nevertheless, we found ecologically significant antibiotic-induced changes in relative abundances that are for the most part consistent between temperature treatments or consistent within the patterns observed in methanogenesis. Regarding the processes of methanogenesis investigated in the present study, the reduction of Methanomicrobia at 10 °C in combination with its increase at 15 and 20 °C (all compared to the antibiotic-free control at the middle of the incubation) provides a mechanistic perspective. This observation matches the pattern we found in CH$_4$ production and is thus a key mechanistic link suggested by our

Fig. 4 | The 15 most expressed transcripts from the KEGG methane metabolism pathway expressed as transcripts per million. Transcriptions of subunits were assigned to the respective enzyme plotted as mean with bootstrapped 95%-confidence intervals alongside raw values. Columns show the different time point, while rows show the different temperatures. Temperature treatments are further distinguished by the hue (i.e., color type, blue: 10 °C; green: 15 °C; yellow: 20 °C) and concentrations of antibiotics by the lightness (light: 0 μg L^{-1}; dark: 5000 μg L^{-1}).

study. Within this class, the genus *Methanosarcina* within the family Methanosarcinaceae is by far the most relevant according to dissimilarities between control and the high antibiotic concentration. This taxon is highly diverse and utilizes almost all known substrates for methanogenesis[61], which complicates defining the methanogenic pathway predominantly responsible for the observed effects on methanogenesis more precisely (but see section "Transcriptional alterations"). Moreover, given the comparatively low relative abundance of Methanomicrobia, their overall contribution to observed assemblage dissimilarities is limited. Furthermore, since we assume that these effects on Methanomicrobia are rather indirectly driven through changes in substrate availability through the metabolic activity of the remaining microbial community and altered chemical environment[10], we discuss the effects on other taxa with a focus on their metabolic capabilities.

The most relevant driver for dissimilarities with up to 100% increases in relative abundance was Clostridia. Within this class, we identified 14 families of which Veillonellaceae (up to 346%), Ruminococcaceae (up to 253%), and Clostridiaceae (up to 211%) showed the highest increases. Their metabolic capabilities are mostly fermentatively converting lactate/lactic acid (Veillonellaceae) and carbohydrates (Veillonellaceae, Ruminococcaceae, Clostridiaceae) into diverse end products

relevant for methanogens (e.g., H$_2$, acetate, and short-chain fatty acids)[62,63]. Other families within the class Clostridia showed notable decreases in response to antibiotics. Among these, reductions by a factor of up to five were observed in the family Syntrophomonadaceae, which is known for a syntrophic relationship with methanogens utilizing H$_2$ and formate[64,65]. Since reductions in response to antibiotics were more pronounced at lower temperatures, this could indicate a relevance for the antibiotic–temperature interaction observed in CH$_4$ production. Because such a trend was less obvious or by tendency inverted (i.e., higher effects at lower temperatures) for the increasing families Veillonellaceae, Ruminococcaceae, and Clostridiaceae, it may be assumed that despite their dominance (up to 52% combined relative abundance) their interaction with Methanomicrobia is comparatively weak. However, as discussed above such binary interactions should be seen as points of reference. Correlational associations should be considered with caution in a microbial assemblage context given that observations in relative abundance are not statistically independent and species interactions are often masked by a common response to an environmental condition (e.g., temperature and antibiotics)[66]. A point which illustrates this is that the largest effects happened in the family Carnobacteriaceae, within the class Bacilli, that is virtually eliminated at the high antibiotic

concentration. These lactic acid bacteria produce substrates relevant for many Veillonellaceae[67] and would thus suggest a reduction of the latter, while the opposite was observed.

Generalizing assemblage responses and their consequences for processing remains a primal research challenge[68]. While both Zhi and Zhang[69] and our study found effects in the relative abundance of *Methanosarcina* and elevated CH_4 production in the presence of antibiotics, the former found weaker effects on the bacterial community, which is contrary to our findings. On the other hand, Mustapha et al.[70] also found the effects of antibiotics on Clostridia and resulting changes in hydrolysis efficiency to be important drivers of increased methanogenesis, which is in line with our findings. In addition, we found increasing relative abundances in the hydrolyzing order Ellin329[71] (up to 882%) within Alphaproteobacteria and the facultative anaerobic family Aeromonadaceae[72] (up to 459%) within Gammaproteobacteria that could alter the hydrolysis efficiency. Wu et al.[7] compiled anaerobic digester studies on a multitude of antibiotics that show both inhibiting and enhancing effects on CH_4 production and numerous taxonomic groups involved. Inducing mechanisms are confounded by the fact that many species cannot be isolated and even if they were, predictions would be complicated by emergent properties in complex communities[73]. Appraising the functional redundancy of many taxa is a further challenge to improve interpretation. For example, both taxa of the above-discussed Clostridia and taxa of the second most important class for between-group dissimilarities (i.e., Bacteroidia) produce substrates for methanogens but show opposite effect patterns. Deriving the substrate availabilities from such metagenomic information is thus intricate. Extending the already diverse and capable methodological toolbox by metabolomics and chemical analyses could, however, pave the way for mechanism-oriented ecological models (e.g., consumer-resource models)[73].

Transcriptional alterations

While during the exponential phase, the expression of MCR at 10 and 15 °C followed the patterns we observed in CH_4 production, no difference was observed at 20 °C. Since metatranscriptome analyses are still extremely cost-intensive we rely on single measurements of a pooled sample. Although effect sizes at least prompt toward an ecological significance of antibiotic alterations, it is possible that between group equivalence is within the natural variability of the sample despite differences in means and vice versa. Nevertheless, the credibility of the patterns in MCR is supported by comparable effect patterns in ACDS complex. This finding furthermore suggests the acetoclastic pathway to be affected since it is responsible for the synthesis (but also cleavage) of acetate[74]. Such reversibility of reactions, however, complicates interpretations. For example, at 10 and 15 °C expression of MCR is higher at steady-state (i.e., the end of the incubation) although CH_4 production is much lower compared to the exponential phase. Although MCR is proposed to track methanogenesis[75], our and other studies found weak correlations between MCR expression and methanogenesis[76], which could for example be influenced by unknown post-transcriptional controls[77]. On the other hand, MCR also catalyzes the reverse process, namely the anaerobic oxidation of CH_4[78,79], which further complicates interpretation. That the elevated MCR levels are to some extent related to anaerobic methanotrophy, would also explain why this was less pronounced at 20 °C. At 20 °C the CH_4 production rates slightly missed our objective a priori criterion to conclude the experiment (i.e., <1% production rate). For this reason, the samples were retrieved at a later successional stage where CO_2 production and thus methanotrophy were less pronounced.

Assessing effects on the hydrogenotrophic pathway is intricate because a multitude of steps and enzymes being involved (indicated by the "hydrolase" suffix). Nevertheless, stable isotope analysis suggests that most CH_4 is produced via the acetoclastic pathway justifying our focus on the latter to address the observed effects of antibiotics.

However, for most enzymes, effects were ambiguous between temperatures and the same line of argument as for the metagenome holds: binary and correlative associations require resolution in order to understand precise drivers of the observed temperature dependence of antibiotic effects on methanogenesis. Nevertheless, in combination with our metabarcoding data we interpret that antibiotics directly affect taxonomic groups responsible for hydrolysis and fermentation, which in turn changed substrate availability and expression of proteins that utilize these substrates (e.g., MCR and ACDS).

Conclusion

The present study shows that the potentially harmful effects of antibiotics on the concentrations of greenhouse gases through an increased methanogenesis can be more relevant at higher temperatures. Furthermore, metabarcoding results underpin this finding with significant shifts in assemblage and species relevant for methanogenesis. Both analyses of the metatranscriptome and stable isotopes suggest acetoclastic methanogenesis to be most prominently affected, which might be indirectly driven by the assemblage's efficiency to hydrolyze substrates. Transferring laboratory results to the field is a core task for continuative research but is complicated by oxidation[80] as well as the effects of antibiotics on oxidation[81]. Nonetheless, field-relevance could be suspected given that systems exposed to chemical stressors (e.g., urban waters and fish ponds) show among the highest CH_4 emissions[82,83]. The findings of this study are a key component to understand the influence of antibiotics on natural CH_4 emissions and more importantly how these effects might contribute to climate change feedbacks. Although further evidence (e.g., for other chemical stressors) and quantitative descriptions are needed to allow generalizations, the current evidence points toward an increasing importance of antibiotic effects on methanogenesis with progressing climate change.

References
1. IPCC. Climate change 2021—the physical science basis. In *Working Group I Contribution to the Sixth Assessment Report of the Intergovernmental Panel on Climate Change* (Cambridge University Press, 2021).
2. Saunois, M. et al. The Global Methane Budget 2000–2017. *Earth Syst. Sci. Data* **12**, 1561–1623 (2020).
3. Conrad, R. Importance of hydrogenotrophic, aceticlastic and methylotrophic methanogenesis for methane production in terrestrial, aquatic and other anoxic environments: a mini review. *Pedosphere* **30**, 25–39 (2020).
4. Oh, Y. et al. Improved global wetland carbon isotopic signatures support post-2006 microbial methane emission increase. *Commun. Earth Environ.* **3**, 159 (2022).
5. Koffi, E. N., Bergamaschi, P., Alkama, R. & Cescatti, A. An observation-constrained assessment of the climate sensitivity and future trajectories of wetland methane emissions. *Sci. Adv.* **6**, eaay4444 (2020).
6. Beaulieu, J. J., DelSontro, T. & Downing, J. A. Eutrophication will increase methane emissions from lakes and impoundments during the 21st century. *Nat. Commun.* **10**, 1375 (2019).

7. Wu, Q. et al. Effects of antibiotics on anaerobic digestion of sewage sludge: performance of anaerobic digestion and structure of the microbial community. *Sci. Total Environ.* **845**, 157384 (2022).

8. Danner, M.-C., Robertson, A., Behrends, V. & Reiss, J. Antibiotic pollution in surface fresh waters: occurrence and effects. *Sci. Total Environ.* **664**, 793–804 (2019).

9. Bollinger, E. et al. Antibiotics as a silent driver of climate change? A case study investigating methane production in freshwater sediments. *Ecotoxicol. Environ. Saf.* **228**, 113025 (2021).

10. Zhang, Z., Xu, Z. & Wang, X. The greenhouse effect of antibiotics: the influence pathways of antibiotics on methane release from freshwater sediment. *Environ. Int.* **176**, 107964 (2023).

11. Wang, J. et al. Effects of florfenicol on methane accumulation and changes in the structure of the prokaryotic community in a water–sediment system. *Sci. Total Environ.* **847**, 157444 (2022).

12. Schulz, S., Matsuyama, H. & Conrad, R. Temperature dependence of methane production from different precursors in a profundal sediment (Lake Constance). *FEMS Microbiol. Ecol.* **22**, 207–213 (2006).

13. Tian, Z., Zhang, Y., Yu, B. & Yang, M. Changes of resistome, mobilome and potential hosts of antibiotic resistance genes during the transformation of anaerobic digestion from mesophilic to thermophilic. *Water Res.* **98**, 261–269 (2016).

14. Hutton, S. J., Siddiqui, S. & Brander, S. M. Ecotoxicology challenges during climate change scenarios. in *Aquatic Ecotoxicology: Understanding Pollutants, Aquatic Organisms, and their Environments* (eds Siddiqui, S. & Brander, S. M.) 147–165 (Springer International Publishing, Cham, 2024).

15. Li, W. et al. Association between antibiotic resistance and increasing ambient temperature in China: an ecological study with nationwide panel data. *Lancet Reg Health West. Pac.* **30**, 100628 (2023).

16. Rodríguez-Verdugo, A., Lozano-Huntelman, N., Cruz-Loya, M., Savage, V. & Yeh, P. Compounding effects of climate warming and antibiotic resistance. *iScience* **23**, 101024 (2020).

17. Cardoso, K. et al. DnaK and GroEL are induced in response to antibiotic and heat shock in *Acinetobacter baumannii*. *J. Med. Microbiol.* **59**, 1061–1068 (2010).

18. Andrade-Linares, D. R., Lehmann, A. & Rillig, M. C. Microbial stress priming: a meta-analysis. *Environ. Microbiol.* **18**, 1277–1288 (2016).

19. Hilker, M. et al. Priming and memory of stress responses in organisms lacking a nervous system. *Biol. Rev.* **91**, 1118–1133 (2016).

20. Rangel, D. E. N. Stress induced cross-protection against environmental challenges on prokaryotic and eukaryotic microbes. *World J. Microbiol. Biotechnol.* **27**, 1281–1296 (2011).

21. Noyes, P. D. et al. The toxicology of climate change: environmental contaminants in a warming world. *Environ. Int.* **35**, 971–986 (2009).

22. O'Reilly, C. M. et al. Rapid and highly variable warming of lake surface waters around the globe. *Geophys. Res. Lett.* **42**, 10773–10781 (2015).

23. Yvon-Durocher, G., Hulatt, C. J., Woodward, G. & Trimmer, M. Long-term warming amplifies shifts in the carbon cycle of experimental ponds. *Nat. Clim. Change* **7**, 209–213 (2017).

24. Holgerson, M. A. & Raymond, P. A. Large contribution to inland water CO_2 and CH_4 emissions from very small ponds. *Nat. Geosci.* **9**, 222–226 (2016).

25. Poole, G. C. & Berman, C. H. An ecological perspective on in-stream temperature: natural heat dynamics and mechanisms of human-caused thermal degradation. *Environ. Manag.* **27**, 787–802 (2001).

26. Fick, J. et al. Contamination of surface, ground, and drinking water from pharmaceutical production. *Environ. Toxicol. Chem.* **28**, 2522 (2009).

27. Lide, D. R. *CRC Handbook of Chemistry and Physics* Vol. 85 (CRC Press, 2004).

28. Weiss, R. F. Carbon dioxide in water and seawater: the solubility of a non-ideal gas. *Mar. Chem.* **2**, 203–215 (1974).

29. Whiticar, M. J. Carbon and hydrogen isotope systematics of bacterial formation and oxidation of methane. *Chem. Geol.* **161**, 291–314 (1999).

30. Walters, W. et al. Improved bacterial 16S rRNA gene (V4 and V4-5) and fungal internal transcribed spacer marker gene primers for microbial community surveys. *mSystems* **1**, e00009-15 (2015).

31. Martin, M. Cutadapt removes adapter sequences from high-throughput sequencing reads. *EMBnet J.* **17**, 10–12 (2011).

32. Callahan, B. J. et al. DADA2: High-resolution sample inference from Illumina amplicon data. *Nat. Methods* **13**, 581–583 (2016).

33. Rognes, T., Flouri, T., Nichols, B., Quince, C. & Mahé, F. VSEARCH: a versatile open source tool for metagenomics. *PeerJ* **4**, e2584 (2016).

34. Edgar, R. C. SINTAX: a simple non-Bayesian taxonomy classifier for 16S and ITS sequences. Preprint at *bioRxiv* https://doi.org/10.1101/074161 (2016).

35. McDonald, D. et al. An improved Greengenes taxonomy with explicit ranks for ecological and evolutionary analyses of bacteria and archaea. *ISME J.* **6**, 610–618 (2012).

36. Bokulich, N. A. et al. Quality-filtering vastly improves diversity estimates from Illumina amplicon sequencing. *Nat. Methods* **10**, 57–59 (2013).

37. Andrews, S. FastQC: a quality control tool for high throughput sequence data. http://www.bioinformatics.babraham.ac.uk/projects/fastqc/ (2010).

38. Ewels, P., Magnusson, M., Lundin, S. & Käller, M. MultiQC: summarize analysis results for multiple tools and samples in a single report. *Bioinformatics* **32**, 3047 (2016).

39. Bolger, A. M., Lohse, M. & Usadel, B. Trimmomatic: a flexible trimmer for Illumina sequence data. *Bioinformatics* **30**, 2114–2120 (2014).

40. Kopylova, E., Noé, L. & Touzet, H. SortMeRNA: fast and accurate filtering of ribosomal RNAs in metatranscriptomic data. *Bioinformatics* **28**, 3211–3217 (2012).

41. Grabherr, M. G. et al. Full-length transcriptome assembly from RNA-Seq data without a reference genome. *Nat. Biotechnol.* **29**, 644–652 (2011).

42. Tamames, J. & Puente-Sánchez, F. SqueezeMeta, a highly portable, fully automatic metagenomic analysis pipeline. *Front. Microbiol.* **9**, 3349 (2019).

43. Grasset, C. et al. An empirical model to predict methane production in inland water sediment from particular organic matter supply and reactivity. *Limnol. Oceanogr.* **66**, 3643–3655 (2021).

44. Richards, F. J. A flexible growth function for empirical use. *J. Exp. Bot.* **10**, 290–300 (1959).

45. R Core Team. *R: A Language and Environment for Statistical Computing* (R Foundation for Statistical Computing, Vienna, Austria, 2023).

46. Bürkner, P.-C. brms: an R package for Bayesian multilevel models using Stan. *J. Stat. Softw.* **80**, 1–28 (2017).

47. Stan Development Team. RStan: the R interface to Stan. R package version 2.32.3, https://mc-stan.org/ (2023).

48. Oksanen, J. et al. Vegan: community ecology package. R package version 2.6-4, https://github.com/vegandevs/vegan (2022).

49. Anderson, M. J. Permutation tests for univariate or multivariate analysis of variance and regression. *Can. J. Fish. Aquat. Sci.* **58**, 626–639 (2001).

50. Puente-Sánchez et al. SQMtools: automated processing and visual analysis of'omics data with R and anvi'o. *BMC Bioinform.* **21**, 1–11 (2020).

51. Cui, M., Ma, A., Qi, H., Zhuang, X. & Zhuang, G. Anaerobic oxidation of methane: an "active" microbial process. *MicrobiologyOpen* **4**, 1–11 (2015).

52. Chebotar, I. V. et al. The classification of bacterial survival strategies in the presence of antimicrobials. *Microb. Pathog.* **155**, 104901 (2021).

53. Lu, X. et al. Long-term effect of the antibiotic cefalexin on methane production during waste activated sludge anaerobic digestion. *Bioresour. Technol.* **169**, 644–651 (2014).

54. Zhou, G., Shi, Q.-S., Huang, X.-M. & Xie, X.-B. The three bacterial lines of defense against antimicrobial agents. *Int. J. Mol. Sci.* **16**, 21711–21733 (2015).

55. Coussens, N. P. & Daines, D. A. Wake me when it's over – bacterial toxin–antitoxin proteins and induced dormancy. *Exp. Biol. Med.* **241**, 1332–1342 (2016).

56. Lenart-Boroń, A., Prajsnar, J., Guzik, M., Boroń, P. & Chmiel, M. How much of antibiotics can enter surface water with treated wastewater and how it affects the resistance of waterborne bacteria: a case study of the Białka river sewage treatment plant. *Environ. Res.* **191**, 110037 (2020).

57. Zhi, S., Li, Q., Yang, F., Yang, Z. & Zhang, K. How methane yield, crucial parameters and microbial communities respond to the stimulating effect of antibiotics during high solid anaerobic digestion. *Bioresour. Technol.* **283**, 286–296 (2019).

58. Alcock, B. P. et al. CARD 2023: expanded curation, support for machine learning, and resistome prediction at the Comprehensive Antibiotic Resistance Database. *Nucleic Acids Res.* **51**, D690–D699 (2023).

59. Yang, Y., Huang, W. & Huang, W. Antibiotic inhibition on anaerobic digestion of animal manure and controlling strategies: a short review. *Clean Soil Air Water* **47**, 1700653 (2019).

60. Canfield, D. E., Kristensen, E. & Thamdrup, B. (eds) Structure and growth of microbial populations. in *Aquatic Geomicrobiology* Vol. 48, 23–64 (Academic Press, 2005).

61. Oren, A. The family Methanosarcinaceae. in *The Prokaryotes* (eds Rosenberg, E. et al.) 259–281 (Springer, Berlin, Heidelberg, 2014).

62. La Reau, A. J. & Suen, G. The Ruminococci: key symbionts of the gut ecosystem. *J. Microbiol.* **56**, 199–208 (2018).

63. Marchandin, H. & Jumas-Bilak, E. The family Veillonellaceae. in *The Prokaryotes* (eds. Rosenberg, E. et al.) 433–453 (Springer, Berlin, Heidelberg, 2014).

64. Schink, B. & Muñoz, R. The family Syntrophomonadaceae. in *The Prokaryotes: Firmicutes and Tenericutes* (eds. Rosenberg, E. et al.) 371–379 (Springer, Berlin, Heidelberg, 2014).

65. Sobieraj, M. & Boone, D. R. Syntrophomonadaceae. in *The Prokaryotes: Volume 4: Bacteria: Firmicutes, Cyanobacteria* (eds. Dworkin, M. et al.) 1041–1049 (Springer, New York, NY, USA, 2006).

66. Carr, A., Diener, C., Baliga, N. S. & Gibbons, S. M. Use and abuse of correlation analyses in microbial ecology. *ISME J.* **13**, 2647–2655 (2019).

67. Lawson, P. A. & Caldwell, M. E. The family Carnobacteriaceae. in *The Prokaryotes: Firmicutes and Tenericutes* (eds. Rosenberg, E. et al.) 19–65 (Springer, Berlin, Heidelberg, 2014).

68. Vanwonterghem, I., Jensen, P. D., Ho, D. P., Batstone, D. J. & Tyson, G. W. Linking microbial community structure, interactions and function in anaerobic digesters using new molecular techniques. *Curr. Opin. Biotechnol.* **27**, 55–64 (2014).

69. Zhi, S. & Zhang, K. Antibiotic residues may stimulate or suppress methane yield and microbial activity during high-solid anaerobic digestion. *Chem. Eng. J.* **359**, 1303–1315 (2019).

70. Mustapha, N. A. et al. Seeking key microorganisms for enhancing methane production in anaerobic digestion of waste sewage sludge. *Appl. Microbiol. Biotechnol.* **102**, 5323–5334 (2018).

71. Harbison, A. B., Carson, M. A., Lamit, L. J., Basiliko, N. & Bräuer, S. L. A novel isolate and widespread abundance of the candidate alphaproteobacterial order (Ellin 329), in southern Appalachian peatlands. *FEMS Microbiol. Lett.* **363**, fnw151 (2016).

72. Lee, C., Kim, J., Hwang, K. & Hwang, S. Fermentation and growth kinetic study of *Aeromonas caviae* under anaerobic conditions. *Appl. Microbiol. Biotechnol.* **83**, 767–773 (2009).

73. Van Den Berg, N. I. et al. Ecological modelling approaches for predicting emergent properties in microbial communities. *Nat. Ecol. Evol.* **6**, 855–865 (2022).

74. Grahame, D. A., Gencic, S. & DeMoll, E. A single operon-encoded form of the acetyl-CoA decarbonylase/synthase multienzyme complex responsible for synthesis and cleavage of acetyl-CoA in *Methanosarcina thermophila*. *Arch. Microbiol.* **184**, 32–40 (2005).

75. Alvarado, A. et al. Microbial trophic interactions and mcrA gene expression in monitoring of anaerobic digesters. *Front. Microbiol.* **5**, 597 (2014).

76. Freitag, T. E. & Prosser, J. I. Correlation of methane production and functional gene transcriptional activity in a peat soil. *Appl. Environ. Microbiol.* **75**, 6679–6687 (2009).

77. Kahnt, J. et al. Post-translational modifications in the active site region of methyl-coenzyme M reductase from methanogenic and methanotrophic archaea. *FEBS J.* **274**, 4913–4921 (2007).

78. Hallam, S. J. et al. Reverse methanogenesis: testing the hypothesis with environmental genomics. *Science* **305**, 1457–1462 (2004).

79. Scheller, S., Goenrich, M., Boecher, R., Thauer, R. K. & Jaun, B. The key nickel enzyme of methanogenesis catalyses the anaerobic oxidation of methane. *Nature* **465**, 606–608 (2010).

80. Bastviken, D., Ejlertsson, J. & Tranvik, L. Measurement of methane oxidation in lakes: a comparison of methods. *Environ. Sci. Technol.* **36**, 3354–3361 (2002).

81. Tong, T. & Xie, S. Impacts of sulfanilamide and oxytetracycline on methane oxidation and methanotrophic community in freshwater sediment. *Ecotoxicology* **28**, 392–398 (2019).

82. Waldemer, C. & Koschorreck, M. Spatial and temporal variability of greenhouse gas ebullition from temperate freshwater fish ponds. *Aquaculture* **574**, 739656 (2023).

83. Wang, G. et al. Intense methane ebullition from urban inland waters and its significant contribution to greenhouse gas emissions. *Water Res.* **189**, 116654 (2021).

Acknowledgements

Author contributions

Eric Bollinger: conceptualization, methodology, software, validation, formal analysis, investigation, writing—original draft, visualization. Paul Schwilden: investigation, writing—review and editing. Foon Yin Lai: investigation, writing—review and editing. Ralf Schulz: resources, funding acquisition, writing—review and editing. Mirco Bundschuh: conceptualization, writing—review and editing, supervision, funding acquisition. Sabine Filker: conceptualization, formal analysis, writing—review and editing, funding acquisition.

Funding

Competing interests

The authors declare no competing interests.

Additional information

Supplementary information The online version contains supplementary material available at
https://doi.org/10.1038/s43247-024-01828-3.

Correspondence and requests for materials should be addressed to
E. Bollinger.

Peer review information *Communications Earth & Environment* thanks
Céline Lavergne and the other, anonymous, reviewer(s) for their contribution
to the peer review of this work. Primary handling editor: Somaparna Ghosh. A
peer review file is available.

Reprints and permissions information is available at
http://www.nature.com/reprints

Publisher's note Springer Nature remains neutral with regard to
jurisdictional claims in published maps and institutional affiliations.